

Bioluminescence Assisted Switching and Fluorescence Imaging (BASFI)

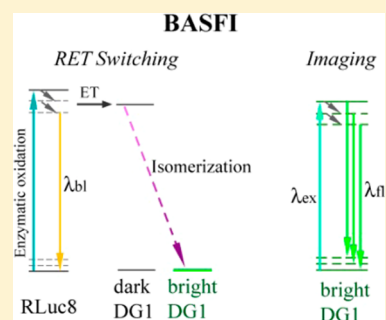
Luyuan Zhang, Fang Xu, Zhixing Chen, Xinxin Zhu, and Wei Min*

Department of Chemistry, Columbia University, New York, New York 10027, United States

S Supporting Information

ABSTRACT: Förster resonance energy transfer (FRET) and bioluminescence resonance energy transfer (BRET) are two major biophysical techniques for studying nanometer-scale motion dynamics within living cells. Both techniques read photoemission from the transient RET-excited acceptor, which makes RET and detection processes inseparable. We here report a novel hybrid strategy, bioluminescence assisted switching and fluorescence imaging (BASFI) using a bioluminescent *Renilla* luciferase RLuc8 as the donor and a photochromic fluorescent protein Dronpa as the acceptor. When in close proximity, RET from RLuc8 switches Dronpa from its original dark state to a stable bright state, whose fluorescence is imaged subsequently with an external laser. Such decoupling between RET and imaging processes in BASFI promises high photon flux as in FRET and minimal bleedthroughs as in BRET. We demonstrated BASFI with Dronpa-RLuc8 fusion constructs and drug-inducible intermolecular FKBP-FRB protein–protein interactions in live cells with high sensitivity, resolution, and specificity. Integrating the advantages of FRET and BRET, BASFI will be a valuable tool for various biophysical studies.

SECTION: Biophysical Chemistry and Biomolecules



Resonance energy transfer (RET) techniques¹ based on fluorescence (FRET)² or bioluminescence (BRET)³ are widely applied for cellular imaging to study fundamental biochemistry. The efficiency of energy transfer is dependent on the sixth order of donor–acceptor distance and hence RET methods are sensitive for short-distance (on the nanometer scale) interactions/changes. Many biochemical interactions/changes fall within this range. Therefore FRET and BRET are well suited for studies of protein–protein interactions^{4,5} as well as protein conformation changes that report functionally important cellular contents such as calcium,⁶ pH,⁷ glucose,⁸ Cu²⁺,⁹ and so forth.

In both FRET and BRET, the photoemission from the RET-excited acceptor serves as the readout. In FRET, an external laser is employed as the energy source for donor excitation (Scheme 1a, left). In BRET, energy source is provided through luciferase substrate oxidation (Scheme 1a, right). Because of the transient nature of the electronic excited state, photoemission of acceptor in both FRET and BRET is collected concurrently as RET occurs.

We here propose a novel hybrid RET strategy, bioluminescence-assisted switching and fluorescence imaging (BASFI), using a bioluminescent donor and a photoswitchable fluorescent protein as its acceptor. Photoswitchable fluorescent proteins such as Dronpa (DG1) are an emerging class of fluorescent proteins that can undergo reversible photoswitching,^{10,11} between a bright fluorescent state and a dark state via chromophore isomerization. This unique property has enabled tremendous advances in frontier imaging techniques, such as super-resolution imaging,¹² deep-tissue imaging,^{13–16} biosen-

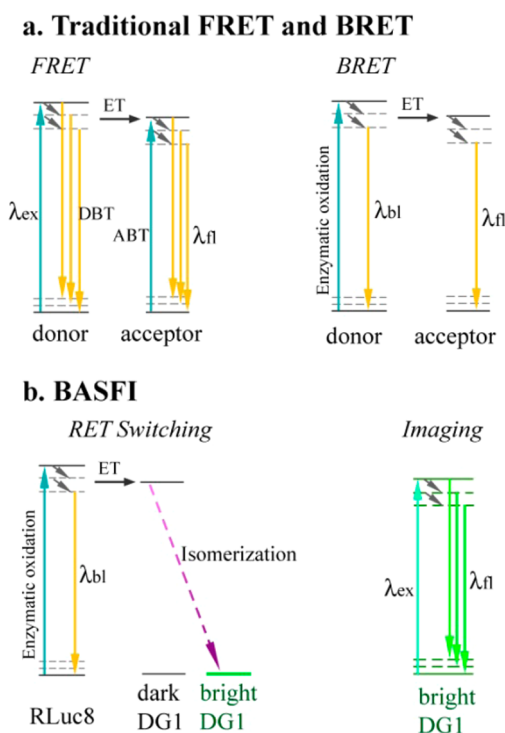
sors,¹⁷ and optical control.¹⁸ Herein we adopt the dark state DG1 as the energy acceptor of a bioluminescent protein RLuc8. The photophysics involved in BASFI is illustrated in Scheme 1(b). Bioluminescence energy transfer from RLuc8 excites the dark-state DG1, which isomerizes to a bright state. This bright state population is thermally stable and does not relax back to dark state. Therefore, as the bioluminescence and RET continues, the population of bright state DG1 accumulates. We subsequently image this bright state population with an external laser that excites the DG1 only. In this way, the RET process and imaging process are temporally decoupled. We demonstrated the principle of BASFI and applied it in imaging of intramolecular and intermolecular protein–protein interactions (PPI). In both cases BASFI can achieve both the high sensitivity of FRET and the minimal spectral bleedthrough of BRET.

As in FRET and BRET, donor and acceptor spectral overlap is critical in BASFI. In equilibrium, DG1 is mainly in its bright state, which emits green fluorescence when excited at 450–550 nm. Blue light around 488 nm can switch DG1 to a stable dark state, which can then be switched back to the bright state by violet light around 400 nm. As the switching-on quantum yield of DG1 is much higher than the switching-off yield, we naturally harness its efficient on-switching process in our BASFI design. To match the absorption spectrum of the DG1 dark state, we specifically chose BRET2^{19,20} enzyme and substrate

Received: October 2, 2013

Accepted: November 1, 2013

Published: November 1, 2013

Scheme 1. Photophysics Involved in FRET, BRET and BASFI^a

^a(a) In FRET, the donor is excited by an external laser, which may fluoresce (DBT) or transfer energy (ET) to the acceptor. The acceptor then will emit photon (λ_{em}). Due to spectral overlap, the acceptor may also be excited by donor excitation laser (ABT). In BRET, donor is excited by enzymatic oxidation of luciferase substrate, which may emit bioluminescence (λ_{bi}) or transfer energy to an acceptor and the acceptor will emit photons. (b) In BASFI, the donor is bioluminescent RLuc8. ET excites dark state DG1, which isomerizes to its bright state. The bright state is subsequently imaged with an external laser that excites DG1 only.

that luminesces around 400 nm as the donor (while the BRET1 system luminesces around 490 nm²¹). After absorbing ET from RLuc8, the dark state of DG1 can be switched to its bright state, which can then be subsequently imaged with an external laser (Scheme 1b).

CTZ400a, also referred to as “deep blue C”, used to be the sole RLuc8 substrate that luminesces around 400 nm. The luminescence quantum yield of CTZ400a is extremely low.^{22,23} We here present three new CTZ analogues, me-CTZ, me-eCTZ, and me-eCTZf, from Nanolight Technology (“me” stands for “methoxy”). Figure 1 shows the RLuc8 catalyzed bioluminescence spectra and kinetics of these four substrates. The spectra all peak around 400 nm with substantial overlaps with the absorption spectrum of the dark state DG1 (Figure 1a). The me- substrates exhibit up to 13-fold higher luminescence than CTZ400a (Figure 1b). Hence they are good candidates for BASFI, as will be shown in the following.

We first demonstrate the effectiveness of BASFI in a fusion construct DG1-RLuc8(S257G). DG1 was fused to the N-terminus of RLuc8 with an optimized 12-amino-acid linker.²⁴ A point mutation S257G was introduced into RLuc8 to increase the luminescence yield.²⁵ We expressed the fusion in HEK293T cells and performed BASFI in live cells. The experimental procedure and raw data are illustrated in Scheme 2. In equilibrium, DG1 is in bright state (Scheme 2a), so we first

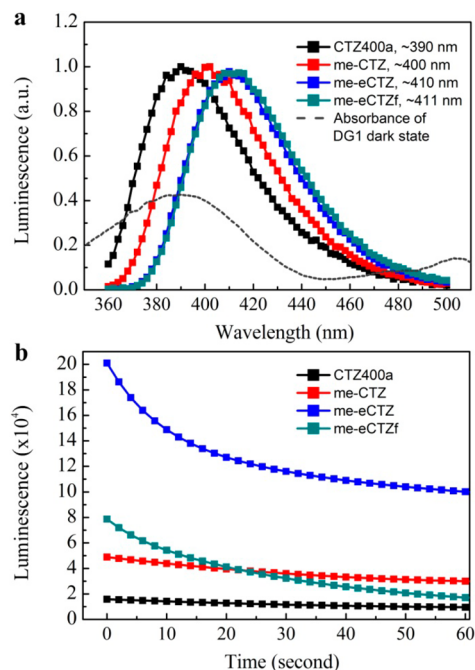
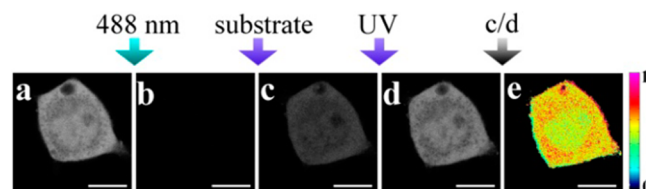


Figure 1. Bioluminescence spectra and reaction kinetics of different substrates catalyzed by RLuc8. Reactions were carried out in cell lysates of RLuc8-expressing HEK293T cells mixed with 5 μ M substrates. (a) Bioluminescence spectra. The peaks of substrates are indicated in the legend. The absorption spectrum of DG1 dark state is also overlaid. (b) Bioluminescence kinetics.

Scheme 2. BASFI Experimental Procedure^a

^a(a) DG1 is in bright state at equilibrium. (b) DG1 is switched off by a 488 nm laser. (c) Addition of RLuc8 substrate switches DG1 to bright state after some time. (d) Exposure to UV light switches all DG1 in the cell to bright state. (e) The ratio between the images in (c) and (d) represents the percentage of DG1 switched on by BASFI. Scale bar: 10 μ m.

switched off DG1 by scanning with a 488 nm laser (Scheme 2b), and then substrates were added to the media. We allowed the reaction to proceed for 10 min, and then imaged the BRET-switched-on population of DG1 with a 514 nm excitation laser (Scheme 2c). In order to quantify the extent of BRET facilitated on-switching, we subsequently switched on all DG1 with a UV lamp and imaged again with the 514 nm laser (Scheme 2d). By comparing these two fluorescence images, we got the BRET-switched-on population percentage of the bright state (Scheme 2e).

Figure 2a–d shows the ratio images of such percentages using various substrates. Consistent with their luminescence spectra and yields, me- substrates switch on DG1 more effectively than CTZ400a. As expected, when no substrate was used, DG1 remained in the dark state (Figure 2e). Figure 2g further shows the time-dependent kinetics of the bright state population every 2 min after addition of substrates, for a total of 10 min.

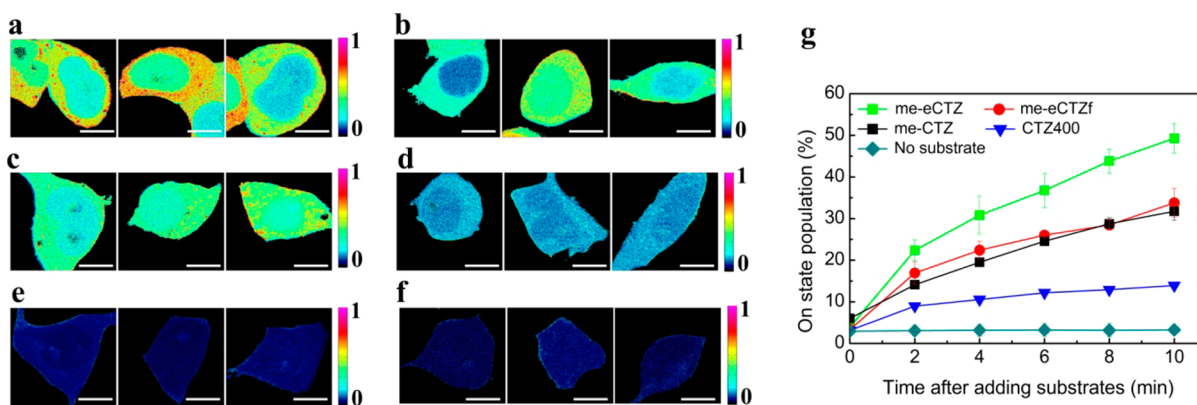


Figure 2. Live cell intramolecular BASFI of DG1-RLuc8(S257G) in HEK293T cells. (a–d): BRET2-switched-on population percentage of DG1 by RLuc8 after incubating with different substrates for 10 min: (a) me-eCTZ; (b) me-eCTZf; (c) me-CTZ; (d) CTZ400a. (e) In the absence of substrates, DG1 stays in the dark state. (f) Control images with DG1 alone expressed in HEK293T cell using me-eCTZ (more control images using other substrates are shown in Figure S1). Without the donor RLuc8, DG1 cannot be switched on. (g) Kinetics of BASFI. Each data point is an average of three cells. The error bars are standard deviation. Scale bar: 10 μm .

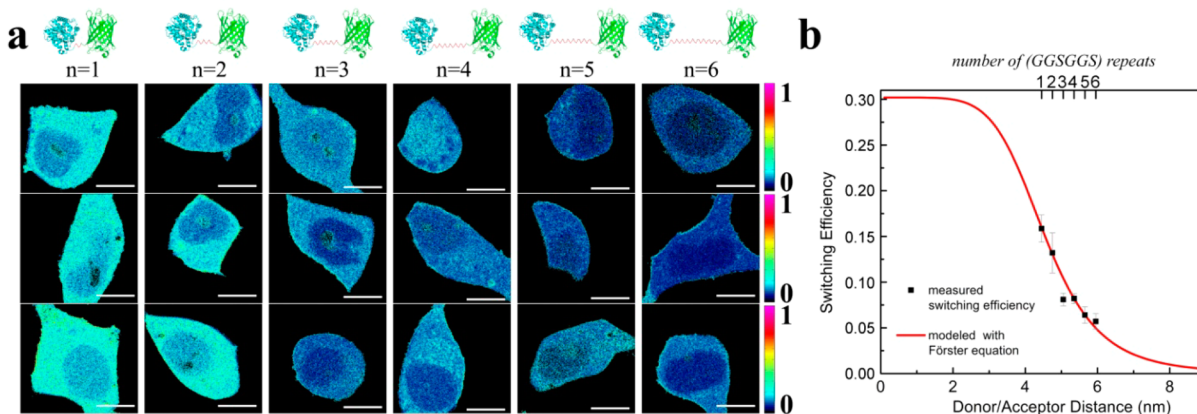


Figure 3. Donor–acceptor distance dependence of BASFI efficiency. (a) Linker length between RLuc8 and DG1 is varied by inserting 1–6 repeats of (GGSGGS) sequence. Three images are shown for each constructs. Substrate used here is 25 μM me-CTZ. Schematic distance change is illustrated on the top. RLuc8 is shown in cyan color and DG1 in green. Red loop is the linker. (b) Measured raw data of BASFI efficiency is modeled with Förster equation to deduce $R_0 = 45 \text{ \AA}$. Three cells are measured for each distance. Error bars are standard deviations. Scale bar: 10 μm .

Both the images and the kinetics of BASFI presented in Figure 2 evidently proved that energy transfer has occurred between RLuc8 and DG1 dark state in our intramolecular construct. When no substrates were present, the measured bright-state population percentage remained below 5%, which arises from the residual dark state fluorescence.¹⁰ When proper substrates were added, bright state population kept increasing as bioluminescence reaction continued. After 10 min, more than 50% DG1 was switched on, yielding a signal-to-background ratio of more than 10. Among the four substrates tested, me-eCTZ outperformed the rest, because of its highest luminescence yield (Figure 1b) and the plausible better spatial orientation between the enzyme-bound me-eCTZ and dark state DG1. For additional controls, we did similar experiments on DG1 alone with me-eCTZ as shown in Figure 2f and other substrates in Figure S1. Without the donor RLuc8, even in the presence of the optimized substrates, DG1 remained in the dark state for all times.

To further validate that the observed fluorescence increase is solely the consequence of BASFI instead of other factors including bioluminescence or DG1 switching-on by long-range scattering luminescence photons, we first performed control experiments with RLuc8 (without DG1) expressed in

HEK293T cell (Figure S2). No signal can be detected when substrates were added to these cells. Therefore the detected signal could not have been bioluminescence. We then coexpressed unlinked RLuc8 and DG1 in HEK293T cells (Figure S3). No significant increase of fluorescence signal was observed after addition of substrates. Therefore when RLuc8 and DG1 are not fused together, no energy transfer occurred between them, and DG1 could not be switched on by scattering bioluminescence photons.

We next determined the interaction range between RLuc8 and DG1. We carried out systematic distance-dependence study of the BASFI efficiency. We fused DG1 to RLuc8 with varying linker lengths. The linkers are (GGSGGS) sequence repeats of 1 to 6 adopted from previous studies.^{26,27} The peptide length increases 3 \AA with every one additional (GGSGGS) sequence as estimated by computer simulation with a worm like chain model.²⁶ We transfected these constructs in HEK293T cells, added 25 μM me-CTZ and measured BASFI efficiency. Ratio images showing BASFI efficiency are shown in Figure 3a. One can see that with increasing linker length, the BASFI efficiency gradually decreases. With 6 data points of BASFI efficiency and estimated distance differences between them, we calculated the Förster

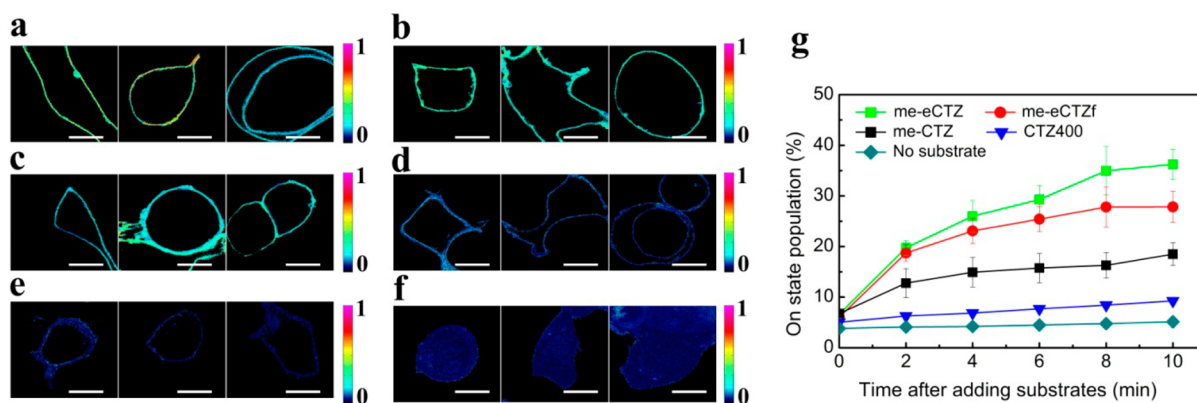


Figure 4. Live cell intermolecular BASFI of Rap induced L-FKBP2-RLuc8 and DG1-FRB association in HEK293T cells. (a–d) Ratio images of BRET2-switched-on population of DG1 after incubating with different substrates for 10 min: (a) me-eCTZ; (b) me-eCTZf; (c) me-CTZ; (d) CTZ400a. (e) Control images without addition of substrates. (f) Control images without Rap, using the substrate me-eCTZ (more control images with other substrates are shown in Figure S4). (g) Kinetics of intermolecular BASFI measured from the membrane region. Each data point is an average of three cells. Error bars are standard deviation. Scale bar: 10 μm .

distance to be 45 Å (Figure 3b) (see Supporting Information for details). This is close to the typical Förster distance between popular GFP FRET pairs.²⁸ It falls within common protein conformation change ranges and protein–protein interaction ranges, which BASFI would be suited for.

Finally we demonstrated that BASFI works well for detection of intermolecular PPI in live cells. As a proof of principle, we chose the well-studied rapamycin (Rap) regulated association of proteins FKBP and FRB as a model system.²⁹ We adopt a chimeric Lyn11-FKBP–FKBP (L-FKBP2) construct that is highly effective in heterodimerization with FRB in the presence of Rap,³⁰ where Lyn11 (L) is a plasma membrane localization sequence. We then fused RLuc8 to the C-terminus of L-FKBP2, and fused DG1 to the N-terminus of FRB. We termed the resulting constructs as L-FKBP2-RLuc8 and DG1-FRB, respectively. We coexpressed L-FKBP2-RLuc8 and DG1-FRB in HEK293T cells. When Rap was present, as shown in Figure 4a–d, after substrates were added, we observed obvious BRET facilitated switching-on of DG1 in the plasma membrane region, which clearly proves that DG1-FRB was attracted to the membrane localized L-FKBP2-RLuc8 and formed heterodimer there. Cytosolic population of DG1 is simply too low to be detected.

As one negative control, in the absence of any substrates but in the presence of Rap, DG1-FRB can be observed on the cell membrane but with extremely low bright-state switching population (Figure 4e). As another negative control, for cells without adding Rap but with substrate me-eCTZ, DG1-FRB is observed to be homogeneously distributed throughout the cytoplasm with no bright-state of DG1 detectable above the baseline (Figure 4f and Figure S4). This observation is consistent with the known fact that Rap is required to induce PPI between FKBP and FRB. Furthermore, Figure 4g shows the detailed kinetics of the bright-state of DG1 every 2 min in the presence of Rap after addition of various substrates. More kinetics curves of control experiments without Rap are shown in Figure S4. DG1 bright state population increases when both Rap and proper substrates are present, but remains below baseline when there is no Rap or substrate. Therefore BASFI demonstrates high specificity in imaging subcellular PPI as exemplified by FKBP and FRB.

We have presented here a novel hybrid RET method, BASFI, that can identify protein–protein interactions in live cells with

high sensitivity, specificity, and resolution. We exploit the transition of DG1 chromophore from dark to bright state on accepting energy around 400 nm. This transition is fundamentally different from those involved in traditional FRET or BRET. In traditional FRET or BRET, energy transfer excites the acceptor to its transient electronic excited state, which quickly returns to its ground state within nanoseconds via spontaneous emission. As a result, the RET-sensitized emission has to be collected simultaneously as the donor excitation and the RET are occurring. In BASFI, energy transfer drives DG1 chromophore isomerization from its dark state to its bright state (both are stable electronic ground states). Unlike the short-lived electronic excited state, the switched-on bright state of DG1 does not relax back to the dark state, and its population steadily accumulates over time as bioluminescence continues. As a result, there is no urgency to image this bright state concurrently as RET occurs. Instead it can be imaged at a later time with an acceptor excitation laser in a fluorescence microscope with high photon flux. Therefore the imaging process is decoupled from the RET process in BASFI.

Such decoupling of RET and imaging in BASFI could significantly reduce spectral bleedthroughs in FRET and elevate photon flux in BRET. As a comparison, we measured the donor and acceptor bleedthroughs in the widely used CFP-YFP FRET pair (Figure S5) and determined donor bleedthrough (DBT) and acceptor bleedthrough (ABT) to be >40% and >10%, respectively. These numbers are much larger than the 5% baseline present in BASFI. Three different samples and seven images are required to correct for these bleedthroughs in FRET. Moreover, typical FRET efficiency is \sim 10% (Figure S5d) and signal-to-background ratio is less than 1. BASFI efficiency is up to 50% and signal-to-background ratio is up to 10. Note that by using photoswitchable fluorescent proteins that have less dark state fluorescence, such as mGeos,³¹ the 5% baseline of DG1 could be further reduced and thus the signal-to-background ratio can be even higher. Meanwhile, external laser excitation of acceptor in BASFI offers much higher photon flux when compared to BRET which is limited by the slow enzyme turnovers. As a result, as demonstrated in FKBP-FRB interaction, BASFI is capable of subcellular imaging, which is difficult to achieve with BRET.

We believe the same strategy should also be applicable to studies of other close-range interactions in live cells such as

protein conformation change, enzymatic dynamics, and so forth. With the future development of more efficient luciferases, brighter substrates, and faster switching fluorescent proteins, we expect that the performance of BASFI could be even more superior.

EXPERIMENTAL METHODS

pcDNA-RLuc8 containing the cDNA of RLuc8 was generously provided by Dr. Sanjiv Sam Gambhir at Stanford University. Plasmid L-FKBP2-CFP and pEGFP-FRB were purchased from Addgene.com. Then L-FKBP2-RLuc8 and DG1-FRB was constructed in GenScript USA, Inc. by replacing the CFP and EGFP with RLuc8 and DG1 gene, respectively. All DG1 and RLuc8 fusion constructs were custom-made in GenScript.

All substrates were purchased from Prolume Ltd. (<http://nanolight.com>). Substrates were dissolved in propylene glycol to a concentration of 5 mM and then stored in a $-80\text{ }^{\circ}\text{C}$ freezer in 1 μL aliquots. To measure the bioluminescence spectra and kinetics, pcDNA-RLuc8 was expressed in HEK293T cell for 48 h, and then was lysed with 1X passive lysis buffer (Promega). Then substrates were added to a final concentration of 5 μM . Luminescence was immediately collected in a BioTek synergy 4 hybrid multimode microplate reader. For the bioluminescence spectra, signal was collected every 2 nm with an integration time of 0.1 s. For the kinetics, signal was collected every 2 s with no filter and an integration time of 1 s.

For BASFI imaging, HEK293T were seeded in Lab-Tek 8-well chambers with glass bottom in a medium composed of 90% DMEM, 10% FBS and 1% penicillin/streptomycin. Plasmids were expressed in HEK293T for 48 h. Then medium was replaced with 1X PBS buffer of pH6.8 right before imaging. Images were collected in Leica TCS SP5 confocal microscope. A 63X 1.2 N.A. water immersion objective was used in all experimental procedures. DG1 was first switched off to the dark state by 5 scans of 488 nm laser with a dwell time of 200 μs . The power of 488 nm laser was 12.7 μW as measure from the front aperture of the objective. Then substrates were manually added into the sample wells to a final 25 μM . Images were taken either every 2 min or after 10 min with a 514 nm laser of 0.7 μW , dwell time 40 μs . Fluorescence of DG1 was collected from 520 to 650 nm. Then sample was shined with the UV lamp for 10 s, and an image of 514 nm excitation was taken again. Images of DG1 population percentage were generated by directly dividing images following addition of substrates to that after exposure to UV.

ASSOCIATED CONTENT

Supporting Information

Details of modeling with Förster equation and additional control data. This material is available free of charge via the Internet at <http://pubs.acs.org>

AUTHOR INFORMATION

Corresponding Author

*E-mail: wm2256@columbia.edu.

Notes

The authors declare no competing financial interest.

ACKNOWLEDGMENTS

We thank Prof. Sanjiv Sam Gambhir for providing pcDNA-RLuc8 plasmid. This work is supported in part by the U.S.

Army Research Laboratory and the U.S. Army Research Office under Contract Number W911NF-12-1-0594.

REFERENCES

- (1) Lohse, M. J.; Nuber, S.; Hoffmann, C. Fluorescence/Bioluminescence Resonance Energy Transfer Techniques to Study G-Protein-Coupled Receptor Activation and Signaling. *Pharmacol. Rev.* **2012**, *64*, 299–336.
- (2) Miyawaki, A. Development of Probes for Cellular Functions Using Fluorescent Proteins and Fluorescence Resonance Energy Transfer. *Annu. Rev. Biochem.* **2011**, *80*, 357–373.
- (3) Welsh, D. K.; Noguchi, T. Cellular Bioluminescence Imaging. In *Cold Spring Harbor Protocols*; Cold Spring Harbor Laboratory Press: Cold Spring Harbor, NY, 2012; Vol. 8; pp 852–866.
- (4) Lowder, M. A.; Appelbaum, J. S.; Hobert, E. M.; Schepartz, A. Visualizing Protein Partnerships in Living Cells and Organisms. *Curr. Opin. Chem. Biol.* **2011**, *15*, 781–788.
- (5) Coulon, V.; Audet, M.; Homburger, V.; Bockaert, J. L.; Fagni, L.; Bouvier, M.; Perroy, J. Subcellular Imaging of Dynamic Protein Interactions by Bioluminescence Resonance Energy Transfer. *Biophys. J.* **2008**, *94*, 1001–1009.
- (6) Miyawaki, A.; Llopis, J.; Heim, R.; McCaffery, J. M.; Adams, J. A.; Ikura, M.; Tsien, R. Y. Fluorescent Indicators for Ca^{2+} Based on Green Fluorescent Proteins and Calmodulin. *Nature* **1997**, *388*, 882–887.
- (7) Esposito, A.; Gralle, M.; Dani, M. A. C.; Lange, D.; Wouters, F. S. pHlameleons: A Family of FRET-Based Protein Sensors for Quantitative pH Imaging. *Biochemistry* **2008**, *47*, 13115–13126.
- (8) Takanaga, H.; Chaudhuri, B.; Frommer, W. B. GLUT1 and GLUT9 as Major Contributors to Glucose Influx in HepG2 Cells Identified by A High Sensitivity Intramolecular FRET Glucose Sensor. *Biochim. Biophys. Acta, Biomembr.* **2008**, *1778*, 1091–1099.
- (9) Kim, H. J.; Park, S. Y.; Yoon, S.; Kim, J. S. FRET-Derived Ratiometric Fluorescence Sensor for Cu^{2+} . *Tetrahedron* **2008**, *64*, 1294–1300.
- (10) Ando, R.; Mizuno, H.; Miyawaki, A. Regulated Fast Nucleocytoplasmic Shuttling Observed By Reversible Protein Highlighting. *Science* **2004**, *306*, 1370–1373.
- (11) Zhou, X. X.; Lin, M. Z. Photoswitchable Fluorescent Proteins: Ten Years of Colorful Chemistry and Exciting Applications. *Curr. Opin. Chem. Biol.* **2013**, *17*, 682–690.
- (12) Shroff, H.; Galbraith, C. G.; Galbraith, J. A.; White, H.; Gillette, J.; Olenych, S.; Davidson, M. W.; Betzig, E. Dual-Color Super-resolution Imaging of Genetically Expressed Probes within Individual Adhesion Complexes. *Proc. Natl. Acad. Sci. U.S.A.* **2007**, *104*, 20308–20313.
- (13) Kao, Y.-T.; Zhu, X.; Xu, F.; Min, W. Focal Switching of Photochromic Fluorescent Proteins Enables Multiphoton Microscopy with Superior Image Contrast. *Biomed. Opt. Express* **2012**, *3*, 1955–1963.
- (14) Zhu, X.; Kao, Y.-T.; Min, W. Molecular-Switch-Mediated Multiphoton Fluorescence Microscopy with High-Order Nonlinearity. *J. Phys. Chem. Lett.* **2012**, *3*, 2082–2086.
- (15) Wei, L.; Chen, Z.; Min, W. Stimulated Emission Reduced Fluorescence Microscopy: A Concept for Extending the Fundamental Depth Limit of Two-Photon Fluorescence Imaging. *Biomed. Opt. Express* **2012**, *3*, 1465–1475.
- (16) Chen, Z.; Wei, L.; Zhu, X.; Min, W. Extending the Fundamental Imaging-Depth Limit of Multi-Photon Microscopy by Imaging with Photo-Activatable Fluorophores. *Opt. Express* **2012**, *20*, 18525–18536.
- (17) Kao, Y.-T.; Zhu, X.; Min, W. Protein-Flexibility Mediated Coupling Between Photoswitching Kinetics and Surrounding Viscosity of a Photochromic Fluorescent Protein. *Proc. Natl. Acad. Sci. U. S. A.* **2012**, *109*, 3220–3225.
- (18) Zhou, X. X.; Chung, H. K.; Lam, A. J.; Lin, M. Z. Optical Control of Protein Activity by Fluorescent Protein Domains. *Science* **2012**, *338*, 810–814.
- (19) Bertrand, L.; Parent, S.; Caron, M.; Legault, M.; Joly, E.; Angers, S.; Bouvier, M.; Brown, M.; Houle, B.; Menard, L. The BRET2/Arrestin Assay in Stable Recombinant Cells: A Platform to Screen for

Compounds That Interact with G Protein-Coupled Receptors (GPCRs). *J. Recept. Signal Transduction Res.* **2002**, *22*, 533–541.

(20) De, A.; Gambhir, S. S. Noninvasive Imaging of Protein–Protein Interactions from Live Cells and Living Subjects Using Bioluminescence Resonance Energy Transfer. *FASEB J.* **2005**, *19*, 2017–2019.

(21) Xu, Y.; Piston, D. W.; Johnson, C. H. A Bioluminescence Resonance Energy Transfer (BRET) System: Application to Interacting Circadian Clock Proteins. *Proc. Natl. Acad. Sci. U. S. A.* **1999**, *96*, 151–156.

(22) Loening, A. M.; Fenn, T. D.; Wu, A. M.; Gambhir, S. S. Consensus Guided Mutagenesis of Renilla Luciferase Yields Enhanced Stability and Light Output. *Protein Eng., Des. Sel.* **2006**, *19*, 391–400.

(23) Loening, A. M.; Wu, A. M.; Gambhir, S. S. Red-Shifted Renilla Reniformis Luciferase Variants for Imaging in Living Subjects. *Nat. Methods* **2007**, *4*, 641–643.

(24) Hoshino, H.; Nakajima, Y.; Ohmiya, Y. Luciferase-YFP Fusion Tag with Enhanced Emission for Single-Cell Luminescence Imaging. *Nat. Methods* **2007**, *4*, 637–639.

(25) Saito, K.; Chang, Y. F.; Horikawa, K.; Hatsugai, N.; Higuchi, Y.; Hashida, M.; Yoshida, Y.; Matsuda, T.; Arai, Y.; Nagai, T. Luminescent Proteins for High-Speed Single-Cell and Whole-Body Imaging. *Nat. Commun.* **2012**, *3*, 1262.

(26) Evers, T. H.; van Dongen, E. M. W. M.; Faesen, A. C.; Meijer, E. W.; Merckx, M. Quantitative Understanding of The Energy Transfer between Fluorescent Proteins Connected via Flexible Peptide Linkers. *Biochemistry* **2006**, *45*, 13183–13192.

(27) van Dongen, E. M. W. M.; Evers, T. H.; Dekkers, L. M.; Meijer, E. W.; Klomp, L. W. J.; Merckx, M. Variation of Linker Length in Ratiometric Fluorescent Sensor Proteins Allows Rational Tuning of Zn(II) Affinity in The Picomolar to Femtomolar Range. *J. Am. Chem. Soc.* **2007**, *129*, 3494–3495.

(28) Lam, A. J.; St-Pierre, F.; Gong, Y.; Marshall, J. D.; Cranfill, P. J.; Baird, M. A.; McKeown, M. R.; Wiedenmann, J.; Davidson, M. W.; Schnitzer, M. J.; et al. Improving FRET Dynamic Range with Bright Green and Red Fluorescent Proteins. *Nat. Methods* **2012**, *9*, 1005–1012.

(29) Chen, J.; Zheng, X. F.; Brown, E. J.; Schreiber, S. L. Identification of an 11-kDa FKBP12-Rapamycin-Binding Domain within The 289-kDa FKBP12-Rapamycin-Associated Protein and Characterization of a Critical Serine Residue. *Proc. Natl. Acad. Sci. U.S.A.* **1995**, *92*, 4947–4951.

(30) Inoue, T.; Do Heo, W.; Grimley, J. S.; Wandless, T. J.; Meyer, T. An Inducible Translocation Strategy to Rapidly Activate and Inhibit Small GTPase Signaling Pathways. *Nat. Methods* **2005**, *2*, 415–418.

(31) Chang, H.; Zhang, M.; Ji, W.; Chen, J.; Zhang, Y.; Liu, B.; Lu, J.; Zhang, J.; Xu, P.; Xu, T. A Unique Series of Reversibly Switchable Fluorescent Proteins with Beneficial Properties for Various Applications. *Proc. Natl. Acad. Sci. U.S.A.* **2012**, *109*, 4455–4460.